Research Article

Development and Application of a Novel Flow-Through Plasma-Activated Water Generator for Household Food Safety: Characterization, Safety, and Antimicrobial Efficacy

Phuthidhorn Thana*, Mathin Jaikua*, Woranika Promsart, Jakkrawut Maitip and Sunisa Ungwiwatkul
Faculty of Science, Energy and Environment, King Mongkut's University of Technology North Bangkok, Rayong Campus, Rayong, Thailand

Dheerawan Boonyawan and Nattawut Palee
Plasma and Beam Physics Research Facility, Department of Physics and Materials Science, Faculty of Science, Chiang Mai University, Chiang Mai, Thailand

Sakhorn Rimjaem
PBP-CMU Electron Linac Laboratory, Plasma and Beam Physics Research Facility, Department of Physics and Materials Science, Faculty of Science, Chiang Mai University, Chiang Mai, Thailand
Research Unit for Development and Utilization of Electron Linear Accelerator and Ultrafast Infrared/Terahertz Laser, Chiang Mai University, Chiang Mai, Thailand

Pichitpon Neamyou
Faculty of Engineering and Technology, King Mongkut's University of Technology North Bangkok, Rayong Campus, Rayong, Thailand

* Corresponding author. E-mail: phuthidhorn.t@sciee.kmutnb.ac.th, mathin.j@sciee.kmutnb.ac.th
DOI: 10.14416/j.asep.2025.09.003
Received: 10 June 2025; Revised: 4 July 2025; Accepted: 16 July 2025; Published online: 12 September 2025

Abstract
Despite the promise of plasma-activated water (PAW) as a chemical-free sanitization approach, its widespread adoption in households is limited by safety concerns and device complexity. This study presents the development of a compact, user-friendly flow-through PAW generator engineered for enhanced safety and antimicrobial performance. Compared to previous designs, the improved system drastically reduces leakage current by 99.6% (from 623 µA to 2.5 µA) and NO_2 gas emissions by 25.7-fold (from 7700 ppb to 300 ppb), ensuring compliance with international safety standards (IEC DIN EN 60601) and air quality regulations (Thailand's NAAQS and the WHO Global Air Quality Guidelines). The antimicrobial efficacy of PAW was demonstrated using raw oyster meat, achieving a 93.5% reduction in total viable count (TVC), equivalent to a 1.19-log reduction, after just two rinse cycles. Importantly, the residual levels of nitrite and nitrate in treated oysters remained well below the acceptable daily intake (ADI) limits established by JECFA. Key technological advancements include a dual-chamber plasma reactor, integrated gas containment, RCBO installation, and optimized electrodes for enhanced plasma stability and reduced risk of electrical leakage. With an energy cost of approximately 0.00192 USD per liter of PAW produced, compact design, and chemical-free operation, this PAW system offers a viable, safe, and environmentally responsible solution for household food decontamination.

Keywords: Antimicrobial efficacy, Electrical safety, Flow-through plasma reactor, Food safety, Non-thermal processing, Plasma-Activated Water (PAW)

1 Introduction

Food safety is a critical global concern, closely linked to public health, economic stability, and food security. Consumption of contaminated food can cause foodborne illnesses, which remain a major global concern [1]. Plasma-activated water (PAW), derived from non-thermal electrical discharge plasma technology, has emerged as a promising non-thermal method to enhance food safety. PAW effectively inactivates pathogenic microorganisms and removes toxins and pesticide residues through reactive oxygen and nitrogen species (RONS) [2]. Its versatility allows application across various food types, regardless of size, shape, or texture [3]–[5].

Although lab-scale PAW studies show great promise, the development of industrial and compact household PAW generators has received limited attention [2]. Additionally, the safety aspects of such systems, especially user exposure to electric shock, UV radiation, reactive radicals, and toxic gas emissions, have not been thoroughly evaluated [6], [7]. These safety considerations are crucial and must be addressed alongside technological development.

Our previous work introduced a compact flow-through PAW generator for household use [8]. This device efficiently produced antibacterial PAW in a single pass with a temperature below 40 °C, suitable for direct application to biological surfaces. This system achieved a 5-log reduction *in vitro* of *Escherichia coli* and *Staphylococcus aureus* within 5 min and significantly reduced *Vibrio cholerae* and *Vibrio parahaemolyticus* in shucked oyster meat by over 86%, highlighting its potential for household food safety.

However, for routine household adoption, this compact PAW generator must meet rigorous safety standards, particularly concerning electrical safety and gas emissions. Like other electrical appliances, plasma-based devices pose a risk of electric shock. Additionally, the plasma reactor generates gaseous by-products like nitric oxide (NO) and nitrogen dioxide (NO_2), which, if not fully dissolved in the PAW, can be released into the atmosphere, causing air pollution and respiratory hazards. Preliminary evaluations of our earlier system revealed leakage currents into the treated water and emission of NO and NO_2 gases, raising health concerns.

This study focuses on further developing the plasma reactor for our compact PAW generator to minimize electric shock hazards and control harmful gas release. We investigated the electrical characteristics of the plasma reactor, monitored leakage currents, and analyzed plasma-generated species in both plasma and gas phases, quantifying pollutant gas emissions. We also assessed the antimicrobial efficacy of the improved PAW system using shucked oyster meat as a representative food substrate and evaluated residual nitrite and nitrate levels to ensure food safety.

2 Materials and Methods

2.1 *The developed flow-through plasma-activated water (PAW) generator system*

Figure 1 illustrates a schematic of the developed flow-through plasma-activated water (PAW) generator system. The figure highlights the internal plasma reactor and the experimental setup used for various measurements, including the voltage–current (V–I) characteristics of the electrical discharge plasma, patient leakage current, identification of plasma-generated species using optical emission spectroscopy (OES) and Fourier-transform infrared (FTIR) spectroscopy, as well as NO_x gas measurement.

The plasma reactor was a closed chamber constructed from poly(methyl methacrylate) (PMMA). Internally, the reactor was divided into two sub-chambers by a partition wall, the lower edge of which was positioned below the water surface. This configuration allowed plasma-activated water to flow from the first sub-chamber to the second through an opening at the bottom of the wall. The partition wall served a critical function by preventing gas generated in the first sub-chamber from diffusing into the second sub-chamber, thereby minimizing gas escape from the reactor along with the plasma-activated water.

The first sub-chamber contained four pairs of plasma-generating electrodes. Each pair comprised a tungsten anode and a stainless steel mesh cathode. The anode electrodes had needle-like, sharpened tips and were vertically mounted using polytetrafluoroethylene (PTFE) fixtures attached to the upper wall of the reactor. The cathode electrodes were formed by coiling stainless steel mesh into cylindrical shapes that surrounded the corresponding anodes, with their lower ends submerged in water. The electrodes were powered by a modular, multi-channel high-voltage DC power supply. The discharge gap, defined as the distance between the lower tips of the anodes and the water surface, was maintained at 1.0 cm. This specific

distance was established through a prior optimization study utilizing the same high-voltage power supply and pin-to-water plasma discharge configuration [8], [9].

The sub-chamber was also equipped with a normally closed gas sampling port, which provided access for extracting gaseous by-products for subsequent analysis. In addition, a gas exchange port connected to a cartridge filter allowed for pressure equalization and gas exchange between the chamber and the external environment. The cartridge filter acted as a safety barrier, preventing the release of potentially hazardous gases into the surrounding atmosphere. In the second sub-chamber, a mesh grounded electrode, also fabricated from stainless steel mesh and formed into a cylindrical shape, was positioned to surround the outlet tube. This grounded electrode acted as a safeguard to prevent electrical leakage from the reactor.

Water was supplied to the plasma reactor from an external reservoir via an adjustable diaphragm pump. The flow rate was controllable, ranging from 100 to 500 mL/min. The water level in the plasma reactor was maintained at 1.0 cm, corresponding to an approximate volume of 100 cm^3 retained within the reactor. As the water passed through the first sub-chamber of the plasma reactor, it was activated by air plasma generated using ambient air present within the sub-chamber as the process gas. The resulting plasma-activated water, enriched with dissolved reactive oxygen and nitrogen species, was then discharged from the outlet of the plasma-activated water generator via gravitational flow.

The newly developed flow-through PAW generator was equipped with a residual current circuit breaker with overcurrent protection (RCBO) integrated into the device to safeguard users against electric shock hazards. In accordance with IEC 61009-1 standards, the RCBO is designed to disconnect the electrical supply to the device within 100 ms when a leakage current exceeding 30 mA is detected.

The water flow rate used for PAW generation in the developed system, applied consistently across all experiments presented in this study, was set at 300 mL/min. This flow rate was selected based on its ability to maximize the concentration of hydrogen peroxide (H_2O_2) in the produced PAW, which in turn enhances the formation of peroxynitrite ($ONOO^-$) and peroxynitrous acid (ONOOH). These two species are key reactive species responsible for the antimicrobial activity of PAW. This is due to H_2O_2 acting as the limiting precursor in the formation of $ONOO^-$ and ONOOH via its reactions with nitrite (NO_2^-) and nitrous acid (HNO_2), respectively [8].

2.2 *Measurement of electrical characteristics and patient leakage current*

The voltage-current (V-I) characteristics of the plasma reactor were investigated using a digital oscilloscope (Hantek DSO2C15; Qingdao Hantek Electronic Co., Ltd., Shandong, China), which has a 150 MHz bandwidth and a 1 GSa/s sampling rate.

The instantaneous discharge voltage, $V(t)$, across the electrodes was measured with a high-voltage probe (P6015A, Tektronix, Inc., Oregon, USA; 75 MHz bandwidth). Concurrently, the discharge current, $I(t)$, was determined by monitoring the voltage drop, $Vs(t)$, across a 2 Ω shunt resistor using a second high-voltage probe (Hantek PP-200, Qingdao Hantek Electronic Co., Ltd., Shandong, China; 200 MHz bandwidth). The average electrical power dissipated in the plasma discharge was then calculated using the provided formula (1):

$$\bar{P} = (1/T)\int_0^T V(t)I(t)dt \quad (1)$$

where T is the period of the voltage waveform.

The total electric power consumption of the flow-through plasma-activated water generator system was measured using a digital multi-function energy meter (TAXNELE DDS662, Yueqing Taixin Electric Co., Ltd., Zhejiang, China).

Currently, PAW generators are not commercially available, and there are no specific electrical safety standards, such as IEC guidelines, that directly apply to them. Therefore, in this study, the patient leakage current, which is defined as the current that flows into the body through direct-contact interfaces like electrodes, is used as a critical safety parameter. To assess this, the measurement setup follows the human body model described in IEC DIN EN 60601-1 [7]. This model consists of an isolated graphite slab, which acts as an electrically conductive contact surface, mounted on a metal enclosure that houses a circuit simulating the electrical impedance of the human body. The equivalent circuit includes a 1 kΩ resistor (R_2) in series with an RC filter composed of a 10 kΩ resistor (R_1) and a 0.015 μF capacitor (C). The human body model was brought into contact with the PAW effluent discharged from the outlet of the plasma reactor. The voltage drop across the capacitor

in the model circuit was measured using a high-voltage probe (Hantek PP-200, Qingdao Hantek Electronic Co., Ltd., Shandong, China; 200 MHz bandwidth). The resulting patient leakage currents can be determined by following formula (2) [10]:

$$I = \left[\sum_{t=0}^{t_{\text{int}}} \frac{|V_C(t)|}{R_2} \cdot \Delta t \right] \cdot f \quad (2)$$

where I is the patient leakage current, V_c refers to the measured voltage drop across the capacitor. The integration time for a single pulse is denoted by t_{int}, while, Δt represents the inverse count rate, and f signifies the pulse repetition rate.

2.3 *Measurement of plasma-generated species in plasma and gas phases*

To identify the different plasma-generated species created in the plasma discharge, we used optical emission spectroscopy (OES). A broad-range spectrometer (model LR1-T from ASEQ Instruments, Vancouver, Canada) was utilized for this general analysis, covering wavelengths from 192 to 887 nm. For improved signal quality, each measurement was an average of 5 individual samplings.

The chemical composition of the gaseous products generated in the plasma reactor was identified using Fourier transform infrared (FTIR) spectroscopy (VERTEX 80v; Bruker Corporation, Massachusetts, United States) with a 10-cm optical path gas cell equipped with KBr windows. Spectra were recorded in the wavenumber range of 4000–500 cm^{-1} at a spectral resolution of 1 cm^{-1}. Gas from the first sub-chamber was drawn for analysis using a peristaltic pump and subsequently delivered to the gas cell.

The concentrations of plasma-generated NO and NO_2 were analyzed using an exhaust gas analyzer (Testo 350; Testo SE & Co. KGaA, Baden-Württemberg, Germany; NO measuring range: 0–300 ppm; NO_2 measuring range: 0–500 ppm). Measurements were conducted for both gases inside the plasma reactor and at a position 30 cm in front of the developed flow-through PAW generator.

2.4 *Characterization of PAW's physicochemical properties*

Tap water was used to produce plasma-activated water (PAW) via the developed flow-through plasma-activated water generator.

The focus of measurements in PAW, produced by the system, was placed on crucial long-lived reactive oxygen and nitrogen species (RONS) known for their antimicrobial properties. Specifically, (NO_2^-), nitrate (NO_3^-), and hydrogen peroxide (H_2O_2) were the species of interest [11]–[13].

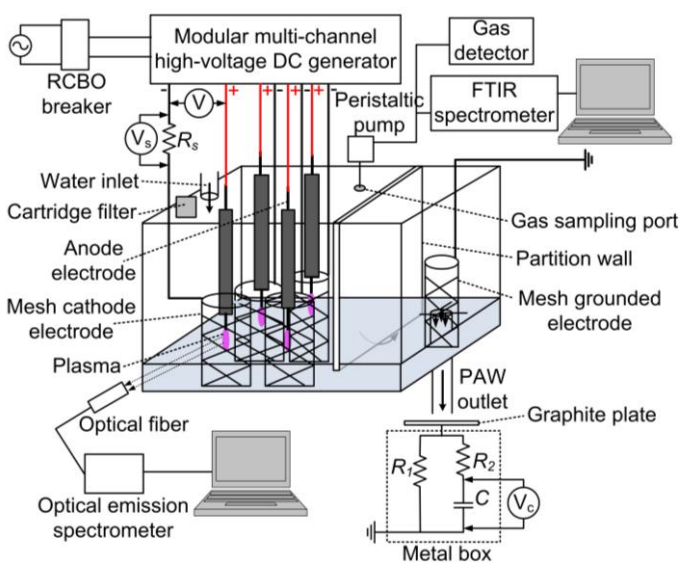

Figure 1: Schematic diagram of the experimental setup detailing the flow-through plasma-activated water (PAW) generator, the plasma reactor, and the systems for measuring electrical characteristics and plasma-generated species.

Quantification of nitrite and nitrate concentrations was carried out using Quantofix® Nitrite/Nitrate test strips (Macherey-Nagel GmbH & Co. KG, North Rhine-Westphalia, Germany). These strips allow for the detection of nitrite levels from 0 to 80 mg/L NO_2^- and nitrate levels from 0 to 500 mg/L NO_3^-. For hydrogen peroxide concentrations, Quantofix® Peroxide 25 test strips (Macherey-Nagel GmbH & Co. KG, North Rhine-Westphalia, Germany) were employed, providing a measurement range of 0 – 25 mg/L.

Furthermore, the physicochemical properties of the PAW, such as pH and temperature, were measured using a portable, pen-type digital meter (AMT03R; Amtast USA Inc., Florida, USA).

2.5 *Evaluation of antimicrobial efficacy and residual nitrite and nitrate levels in PAW-treated shucked oyster meat*

To evaluate the antimicrobial efficacy of PAW treatment on foodborne pathogens, the total viable count (TVC) method was employed. Shucked oyster meat was used as the model sample, consistent with previously published work [8]. The study compared the effectiveness of washing oyster meat with PAW versus sterile distilled water (SDW) and investigated the impact of single versus double washing cycles. For microbial enumeration, the samples were serially diluted and plated on nutrient agar prepared from nutrient broth (HiMedia, M002-500G; HiMedia Laboratories LLC, Pennsylvania, United States) to determine the total viable count.

Shucked oyster meat (*Saccostrea commercialis*) was obtained from a local seafood market in Rayong, Thailand. For each treatment condition, 25 g of oyster meat was immersed in 100 mL of either PAW or SDW for 10 min. For the double-washing condition, this step was repeated.

After washing, the oyster samples were transferred into 225 mL of 0.1% peptone water and homogenized using a Stomacher blender at 100 rpm for 30 s. The resulting solution was then serially diluted using sterile saline solution and spread onto agar culture plates. The plates were subsequently incubated for 24 hours at 37 °C. All colonies were enumerated, and the microbial load was expressed as CFU/g.

The quantification of residual nitrite and nitrate in shucked oyster meat was conducted by the Food and Nutrition Laboratory, Institute of Nutrition, Mahidol University, Nakhon Pathom, Thailand. Oyster meat samples, both untreated and treated with PAW for 10 min with two cleaning cycles (250 g per condition), were submitted for analysis. Residual nitrite content was determined using an in-house method based on ISO 2918:1975, while residual nitrate content was analyzed using an in-house method based on ISO 3091:1975.

2.6 *Statistical analysis of experimental data*

Experiments were performed in triplicate, at a minimum, and the outcomes are presented as the mean ± standard deviation (SD). For data analysis, IBM SPSS Statistics version 28 was utilized.

To identify significant differences between treatment groups, a one-way analysis of variance (ANOVA) was applied. Subsequent post hoc comparisons of group means were conducted using Tukey's Honestly Significant Difference (HSD) test. Statistical significance was set at a p-value less than 0.05 (p-value < 0.05).

3 Results and Discussion

3.1 *Electrical characteristics*

Powering the plasma generator electrodes with a high-voltage DC source initiated an electrical discharge plasma between the tungsten anode tip and the water surface. The water surface functioned as a liquid electrode, connected to a stainless steel mesh cathode. The discharge gap, the distance from the lower tip of the anode rod to the water surface, was set at 1 cm. The observed plasma discharge exhibited characteristics consistent with those documented in previous studies [8], [9]. The V-I characteristics of this plasma discharge are presented in Figure 2.

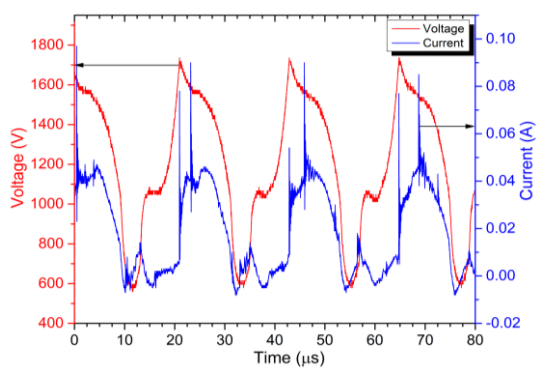

Figure 2: Representative voltage-current characteristics of the electrical discharge plasma within the developed plasma reactor (1 cm discharge gap).

Despite the use of a constant DC power supply for plasma generation, the discharge displayed inherent pulsing behavior. This self-pulsing phenomenon is a common observation across various electrode geometries and discharge modes [14], [15]. For this study, the repetition rate of the electrical discharge pulses was approximately 45 kHz.

The average electrical power dissipated during a single period of plasma discharge was calculated from Equation (1), utilizing the measured V-I waveforms. For discharges generated using electrode pairs 1, 2, 3, and 4, the pulse-average dissipated powers were determined to be 25.8 W, 25.4 W, 26.3 W, and 25.9 W, respectively. The cumulative power dissipation from all plasma discharges within the plasma reactor amounted to 103.4 W. Concurrently, the total electrical power consumption of the entire flow-through plasma-activated water generator system was 268.4 W.

3.2 *Plasma-generated species in plasma and gas phases*

In the discharge region, collisions with energetic free electrons primarily initiated the excitation, ionization, and dissociation of the parent species N_2, O_2, and H_2O. Following the ignition of the plasma discharge, various physical and chemical interactions within this region led to the formation of numerous species [8], [9]. Some of these, such as excited N_2 molecules, atomic nitrogen (N), atomic oxygen (O), atomic hydrogen (H), and hydroxyl (OH) radicals, could be observed via optical emission spectroscopy (OES).

The broadband emission spectrum resulting from the plasma discharge in the reactor of the compact flow-through plasma-activated water system is presented in Figure 3. The second positive system (SPS) of N_2, corresponding to the electronic transition $C^3\Pi_u \rightarrow B^3\Pi_g$, was identified within the 296.2 – 405.9 nm range, while the first positive system (FPS), involving the transition $B^3\Pi_g \rightarrow A^3\Sigma_u^+$, was observed between 590.6 and 760.9 nm [16], [17]. In addition, emission peaks attributed to the first negative system (FNS) of N_2^+, corresponding to the transition $B^2\Sigma_u^+ \rightarrow X^2\Sigma_g^+$, were detected within the 291.4–427.8 nm range [17]. These findings indicate that excited nitrogen species dominate the plasma region. Such species—including $N_2(A^3\Sigma_u^+)$, $N_2(B^3\Pi_g)$, $N_2(C^3\Pi_u)$, and N_2^+—are primarily produced through electron impact excitation and ionization of neutral nitrogen molecules [18], [19].

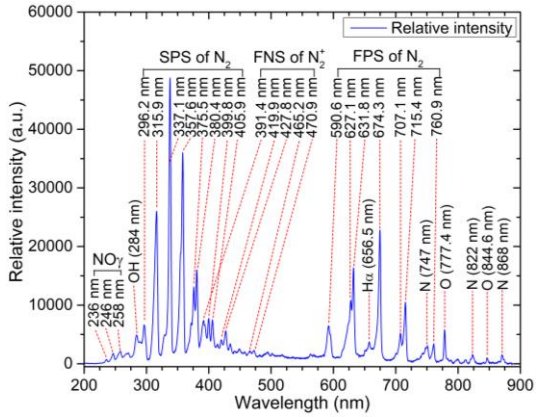

Figure 3: Typical optical emission spectrum of the air plasma discharge within the developed plasma reactor.

Moreover, emission peaks near 236 nm, 246 nm, and 258 nm were attributed to the γ-band transitions of nitric oxide (NO), specifically the $A^2\Sigma^+ \rightarrow X^2\Pi$ transition [20]. The spectrum also revealed the presence of other reactive species, such as hydroxyl radicals (OH, around 284 nm), atomic hydrogen (Hα at 656.45 nm), atomic oxygen (O at 777.4 and 844.6 nm), and atomic nitrogen (N at 747, 822, and 868 nm) [21]–[25].

The various species generated by this plasma discharge can interact with each other, leading to the formation of new RONS groups. The proposed mechanisms for the generation of RONS within the developed plasma reactor of the flow-through PAW generator have been presented in a previously published study [8]. Among these products, long-lived RONS gases, including ozone (O_3), hydrogen peroxide (H_2O_2), nitric oxide (NO), nitrogen dioxide (NO_2), nitrous oxide (N_2O), dinitrogen pentoxide (N_2O_5), nitrous acid (HNO_2), and nitric acid (HNO_3), are particularly stable and can be effectively detected using Fourier-transform infrared (FTIR) spectroscopy [26]–[29].

Figure 4 shows the FTIR spectrum of gases produced in the developed plasma reactor. The analysis identified several long-lived RONS with their characteristic absorption bands include HNO_2, with absorption bands at 3630–3545 cm^{-1} and 890–760 cm^{-1}; NO_2, at 1660–1560 cm^{-1} and 2935–2845 cm^{-1}; N_2O, between 2265–2145 cm^{-1}; NO, in the range of 1965–1770 cm^{-1}; HNO_3, with a peak at 1325 cm^{-1}; and N_2O_5, showing characteristic peaks 569 cm^{-1} [26], [29].

Nevertheless, precise identification of individual gas species was challenging within certain wavenumber ranges due to the interference of absorption bands

from multiple gases. For example, in the 1330–1210 cm^{-1} region, the infrared absorption peak of N_2O overlapped with those of HNO_2 and N_2O_5. Similarly, in the 1735–1670 cm^{-1} range, the absorption band of HNO_2 overlapped with that of N_2O_5 [26].

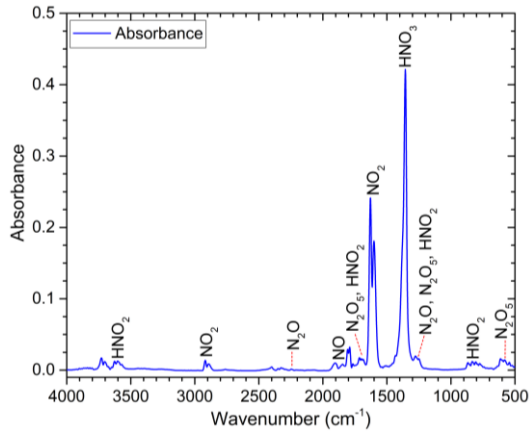

Figure 4: Representative FTIR absorption spectrum of gaseous products generated within the developed plasma reactor.

FTIR spectroscopy of the gases generated within the developed plasma reactor indicated that the long-lived RONS gases formed were predominantly reactive nitrogen species (RNS). We observed a notable absence of significant long-lived reactive oxygen species (ROS) such as ozone (O_3) and hydrogen peroxide (H_2O_2). O_3, typically formed from the reaction between atomic oxygen and oxygen molecules ($O + O_2 + M \rightarrow O_3 + M$, where M is any other species) [27], has a primary infrared absorption peak at 1042 cm^{-1} [26]. H_2O_2, usually resulting from the recombination of hydroxyl radicals ($OH + OH \rightarrow H_2O_2$; $OH + OH + M \rightarrow H_2O_2 + M$) [30], [31], absorbs in the 1170–1380 cm^{-1} range [31], [32].

This absence of O_3 and H_2O_2 is likely due to their very limited formation within the reactor, or, more significantly, their rapid consumption in chemical reactions with other RONS species already present, leading to the formation of new RNS. For instance, O_3 can undergo oxidation reactions with N, NO, and NO_2 to form NO, NO_2, and NO_3, respectively ($N + O_3 \rightarrow NO + O_2$; $NO + O_3 \rightarrow NO_2 + O_2$; $NO_2 + O_3 \rightarrow NO_3 + O_2$) [33], [34]. Meanwhile, H_2O_2 can react with OH and O to produce hydroperoxyl radical, HO_2 ($OH + H_2O_2 \rightarrow HO_2 + H_2O$; $O + H_2O_2 \rightarrow HO_2 + OH$). This HO_2 can then further react with NO to form NO_2 or HNO_3 ($NO + HO_2 \rightarrow NO_2 + OH$; $NO + HO_2 \rightarrow HNO_3$) or with NO_2 to form HNO_2 ($NO_2 + HO_2 \rightarrow HNO_2 + O_2$) [18], [19].

In addition to measuring the gases produced within the developed plasma reactor using an FTIR spectrometer, we utilized a gas analyzer to detect the quantities of NO and NO_2 generated inside the reactor. The average concentrations of these two radicals were found to be 387.3 ± 100.4 ppm and 22.0 ± 7.4 ppm, respectively.

Beyond the two previously mentioned causes concerning the absence of O_3 and H_2O_2, another possible explanation exists. The plasma-generated O and OH radicals, essential precursors for the formation of O_3 and H_2O_2, respectively, appear to have been almost entirely consumed. This consumption occurred in chemical reactions linked to the formation of reactive nitrogen species (RNS) such as NO, NO_2, HNO_2, and HNO_3 within the plasma reactor. Specifically, O radicals react with N_2 to form NO ($O + N_2(A^3\Sigma_u^+) \rightarrow NO + N$), and subsequently with NO to produce NO_2 ($O + NO + M \rightarrow NO_2 + M$). Likewise, OH radicals can be involved in reactions such as with atomic N to form NO ($OH + N \rightarrow NO + H$), with NO to form HNO_2 ($OH + NO + M \rightarrow HNO_2 + M$), and with NO_2 to form HNO_3 ($OH + NO_2 + M \rightarrow HNO_3 + M$) [18], [33].

3.3 *Physicochemical characteristics of PAW*

The physicochemical properties of PAW, produced using the developed flow-through PAW generation system, are presented in Table 1. The system utilized tap water with initial temperature, pH, electrical conductivity (EC), and oxidation-reduction potential (ORP) values of 29.1 ± 0.3 °C, 7.50 ± 0.01, 2 ± 0 µS/cm, and 254 ± 1 mV, respectively. A water flow rate of 300 mL/min was maintained during the PAW generation process.

Table 1: Physicochemical characteristics of plasma-activated water (PAW) generated by the developed flow-through PAW generator.

Parameter	Value
Temperature	33.4 ± 0.6 °C
pH	3.75 ± 0.23
Electrical conductivity (EC)	326 ± 4 µS/cm
Oxidation-reduction potential (ORP)	300 ± 3 mV
Nitrite (NO_2^-)	26.6 ± 5.7 mg/L
Nitrate (NO_3^-)	150.0 ± 43.3 mg/L
Hydrogen peroxide (H_2O_2)	9.2 ± 1.4 mg/L

The PAW produced by our developed PAW generator system has a temperature not exceeding 40 °C.

This crucial characteristic enables the immediate application of the nascent PAW to soft matter, including biological tissues, without inducing thermal damage [35].

Based on the measurements of reactive oxygen and nitrogen species (RONS) in the gas phase within the developed plasma reactor, as presented in Section 3.2, and considering the chemical reactions occurring at the gas-liquid interfacial areas alongside Henry's Law solubility coefficients [18], [36], we hypothesize the following formation mechanisms for the long-lived RONS detected in the PAW generated by our developed system, specifically NO_2^-, NO_3^-, and H_2O_2.

We believe that NO_2^- and NO_3^- originate from the dissociation of HNO_2 and HNO_3, respectively ($HNO_2 \rightarrow NO_2^- + H^+$; $HNO_3 \rightarrow NO_3^- + H^+$). This dissociation not only produces nitrite and nitrate but also generates H^+, leading to the acidic nature of PAW. Both gaseous HNO_2 and HNO_3, found in the plasma reactor, exhibit high Henry's law solubility coefficients (approximately 4.8×10^{-1} mol m^{-3} Pa^{-1} and 2.1×10^{3} mol m^{-3} Pa^{-1}, respectively) [18]. This indicates that gaseous HNO_2 and HNO_3 can readily dissolve in water and subsequently dissociate into NO_2^- and NO_3^-.

Beyond the direct dissolution and dissociation of gaseous HNO_2 and HNO_3, NO and NO_2 also play a role in generating NO_2^- and NO_3^- through chemical reactions that produce HNO_2 and HNO_3. NO and NO_2, detected by both FTIR spectrometer and a gas analyzer, have very low solubility coefficients (approximately 1.9×10^{-5} mol m^{-3} Pa^{-1} and 1.2×10^{-4} mol m^{-3} Pa^{-1}, respectively) [18]. While this implies minimal dissolution in water, these gases can still react with water at the interface to form additional HNO_2 and HNO_3 ($NO + NO_2 + H_2O \rightarrow 2HNO_2$; $2NO_2 + H_2O \rightarrow HNO_2 + HNO_3$) [37].

Regarding the H_2O_2 formation in the PAW, we were unable to detect gaseous H_2O_2 using Fourier Transform Infrared (FTIR) spectroscopy. This suggests that the concentration of H_2O_2 in the gas phase is very low. Consequently, we propose that the majority of H_2O_2 observed in the PAW, produced using a pin-to-water plate electrode geometry, primarily results from the recombination of hydroxyl radicals.

These OH radicals are formed at the gas-liquid interface through charge transfer collisions. Specifically, positive ions generated in the plasma, such as $N_2^+$and N^+, collide with water molecules at the liquid surface. This collision transfers charge to the water molecules, creating water cations, H_2O^+ ($X^+ + H_2O \rightarrow X + H_2O^+$, where X is any species present within the plasma reactor). These water cations subsequently react with surrounding water molecules to yield OH radicals and H_3O^+ ($H_2O^+ + H_2O \rightarrow OH + H_3O^+$) [38].

Both the ·OH radicals and the H_2O_2 resulting from their recombination at the interfacial region exhibit high solubility coefficients (approximately 3.8×10^{-1} mol m^{-3} Pa^{-1} for OH and 9.0×10^{2} mol m^{-3} Pa^{-1} for H_2O_2), enabling their rapid dissolution into the aqueous phase [18].

3.4 *Antimicrobial efficacy of PAW treatment on shucked oyster meat*

To compare the effectiveness of PAW as a cleaning agent versus sterile distilled water (SDW), and to investigate the effect of the number of washing cycles, we employed the total viable count (TVC) method to evaluate the microbial load in shucked oyster meat samples cleaned with PAW and SDW. Shucked oyster meat was selected as a representative raw food commonly consumed in Thailand, which is often associated with foodborne pathogen contamination.

The efficacy of PAW generated by the flow-through PAW generation system and used immediately post-generation, is presented in Table 2.

Table 2: Aerobic plate count in shucked oyster meat samples after treatment with plasma-activated water (PAW) and sterile distilled water (SDW). 1x and 2x denote washing with 100 mL of the respective cleaning agent for 10 min per cycle, for one and two cycles, respectively. Lowercase letters (a–c) indicate statistically significant differences; different letters denote significant differences at p-value < 0.05.

Treatment Condition	Total Viable Count (CFU/g)	Percentage Reduction (%)
Untreated	474.67 ± 16.65^{a}	-
1x SDW-treated	404.00 ± 18.33^{b}	14.9
2x SDW-treated	341.33 ± 44.24^{b}	28.1
1x PAW-treated	94.67 ± 16.65^{c}	80.1
2x PAW-treated	30.67 ± 14.05^{c}	93.5

When shucked oyster meat samples were submerged in either PAW or SDW for 10 min, followed by decanting, a single rinse with PAW significantly reduced the TVC in the oyster meat. This one-time PAW wash achieved an 80.1% reduction in microbial load, which was significantly higher than the 14.9% reduction observed with SDW.

Furthermore, a second rinse with the respective cleaning agents further enhanced the reduction in total viable microbial cells. The reduction increased to 93.5% for PAW-treated samples and 28.1% for SDW-treated samples.

To evaluate the safety implications of these findings, the observed microbial loads were compared with relevant food safety standards. According to the Microbiological Quality Criteria for Food and Food Contact Containers, 3rd Edition (B.E. 2560), published by the Department of Medical Sciences, Ministry of Public Health, Thailand, the permissible limit for TVC in raw oyster meat is 5×10^5 CFU/g. In our study, the microbial loads under various treatment conditions were as follows: untreated (474.67 CFU/g), 1x SDW-treated (404.00 CFU/g), 2x SDW-treated (341.33 CFU/g), 1x PAW-treated (94.67 CFU/g), and 2x PAW-treated (30.67 CFU/g). All treatments resulted in TVC levels well below the regulatory limit. However, the use of PAW significantly enhanced microbial reduction compared to SDW, suggesting its potential as a more effective and safer alternative for decontaminating raw oysters. These findings support the applicability of PAW in improving the microbiological safety of raw seafood in alignment with national food safety standards.

The antimicrobial capability of PAW produced from the developed flow-through PAW generator is likely attributed to peroxynitrite ($ONOO^-$), which is formed from the combination of NO_2^- and H_2O_2 ($NO_2^- + H_2O_2 + H^+ \rightarrow ONOOH + H_2O$, $ONOOH \leftrightarrow ONOO^- + H^+$) [18], [39]. These reactive nitrogen species are well-established to play a crucial role in inactivating a broad spectrum of microorganisms, including bacteria, fungi, and viruses [40]–[43].

Based on our previous study, foodborne pathogenic bacteria commonly found in shucked oyster meat include *Staphylococcus aureus*, *Salmonella* spp., *Vibrio cholerae*, and *Vibrio parahaemolyticus* [8], Peroxynitrite ($ONOO^-$) is known to induce bacterial cell death through both apoptotic and necrotic pathways [11], [44]. Its antimicrobial activity involves lipid peroxidation of microbial membranes, leading to structural disruption [41]. Furthermore, $ONOO^-$ can penetrate bacterial cells and accumulate intracellularly, where it causes extensive damage, including DNA modification, lipid peroxidation, protein oxidation and nitration, and enzyme inactivation, ultimately resulting in bacterial death [11], [45], [46].

Furthermore, the abundance of reactive nitrogen species, such as NO_2^- and NO_3^-, in the PAW generated by this system enhances its effectiveness against foodborne pathogens like *S. aureus* and *E. coli* [42].

Despite PAW generated by the developed flow-through PAW generation system demonstrated excellent microbial reduction in this study and its acidic nature plays a crucial role in enhancing antimicrobial activity [47], [48], the relatively low pH (3.75) of the PAW used may raise concerns regarding potential impacts on the sensory attributes of raw oysters, such as appearance, texture, and flavor. Numerous studies have reported that the undesirable effects of acidic PAW and plasma-activated solutions (PAS), particularly those generated using air plasma, on the quality attributes of various seafood and meat products are generally minimal and depend on the product type [1]. For instance, Qian *et. al*., [48] found that treatment with acidic PAW and plasma-activated lactic acid caused no noticeable changes in the basic properties of beef, including surface color, pH, lipid oxidation, odor, and protein content. However, when applied to chicken drumsticks, a slight reduction in surface redness was observed [49]. For aquatic products, Zhao *et. al*., [50] demonstrated that decontamination of mackerel fillets using plasma-activated peracetic acid with a pH of approximately 2.8 did not result in significant alterations in surface color or other quality parameters. Similarly, Liu *et. al*., [51] reported that acidic PAW caused no significant changes in the sensory properties of yellow river carp fillets.

It is also worth noting that acidic solutions with similar or even lower pH values are widely used in the meat industry for microbial decontamination. For instance, organic acids such as lactic, malic, and fumaric acids are widely employed as antimicrobial washes for meat and poultry carcasses to reduce bacterial contamination [52]–[54]. These applications, despite the low pH of the solutions, have been shown to effectively reduce pathogens with minimal or acceptable effects on the sensory quality, including texture and color, of the treated products [55].

Nevertheless, considering that oysters are consumed raw and are particularly sensitive to sensory alterations, further investigation is needed to assess consumer acceptability and potential sensory alterations following PAW treatment.

3.5 *Device risk assessments*

3.5.1 Patient leakage current

The plasma reactor in flow-through plasma-activated water (PAW) generators presents a potential risk of electrical leakage to the user, similar to hazards found in conventional electric water heaters or other household appliances. This danger is heightened by PAW's relatively high electrical conductivity, which increases its capacity to transmit any leaked current to individuals touching the water as it exits the reactor. Exposure to such leakage currents can cause a range of adverse effects on the human body, from a mild tingling sensation to the stimulation of muscles and nerves, resistive heating of tissues, electrochemical burns, or even electric shock, potentially leading to cardiovascular collapse [7], [10].

Figure 5 displays a representative voltage pulse measured from the equivalent circuit of human body impedance, which was subjected to contact with PAW flowing from the developed plasma reactor's outlet. The measured voltage exhibited an alternating current (AC) pulse characteristic with a repetition rate of approximately 38.5 kHz. Based on Equation (2), the calculated average patient leakage current was 2.5 µA, which is less than the 10 µA threshold current for AC, as specified by IEC DIN EN 60601 [7]. Furthermore, the RCBO breaker installed in the developed flow-through PAW generator, as depicted in Figure 1, did not trip. This indicates that the leakage current from the device did not exceed 30 mA.

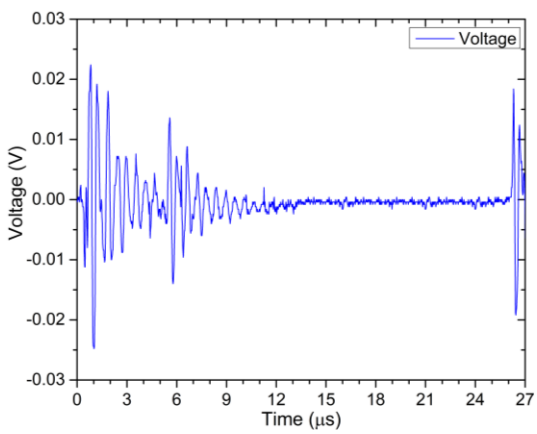

Figure 5: A representative voltage pulse measured across the human body impedance model, used to evaluate the patient leakage current of the reactor.

In comparison, the previous version of the flow-through PAW generator, as presented in our earlier study [8], exhibited a significantly higher leakage current of 623 µA. This quantitative reduction in leakage current demonstrates a substantial safety improvement in the redesigned system, ensuring that the developed PAW generator complies with both medical and household electrical safety standards.

3.5.2 NO_2 emission

Nitrogen dioxide (NO_2) generated within the developed plasma reactor may be released or leaked into the surrounding atmosphere. Such emissions contribute to ambient air pollution and pose significant respiratory health risks [56]. Vulnerable populations, which include individuals with asthma, children, and the elderly, are particularly susceptible to the adverse health effects of NO_2 exposure. The World Health Organization (WHO), along with environmental protection agencies worldwide, recognizes NO_2 as a key indicator pollutant and includes it as a primary metric for assessing overall air quality. According to the WHO Global Air Quality Guidelines (AQGs) 2021, the recommended maximum exposure limit for NO_2 is 13.3 ppb based on a 24-hour mean. In comparison, Thailand's National Ambient Air Quality Standards (NAAQS) set the maximum allowable concentration of NO_2 at 170 ppb for a 1-hour averaging period.

The concentration of NO_2 in the ambient air around the flow-through PAW generator was measured at a distance of 30 cm from the front of the device, approximating the typical user's working distance. Measurements were taken over a 20-min operating period, which corresponds to the production of 6 L of PAW. The average NO_2 concentration recorded was 300 ± 200 ppb. Assuming continuous exposure for the full 20 min, the estimated 1-hour and 24-hour time-weighted average exposures to NO_2 would be 100 ppb and 4.2 ppb, respectively. These values fall below the 1-hour ambient air quality standard set by the Thai government (170 ppb) and the 24-hour guideline recommended by the WHO (13.3 ppb), suggesting acceptable short-term safety for users.

In contrast, the previous version of the flow-through PAW generator, as reported in our earlier study [8], emitted NO_2 at an average concentration of 7700 ± 1000 ppb during operation—more than 25.7 times higher than the current design. This substantial reduction in NO_2 emissions reflects a major improvement in emission control and represents a

significant advancement in user and environmental safety.

Nonetheless, despite the lower emissions from the current system, strategies to further minimize user exposure remain beneficial. These include enhancing the device's NO_2 capture or conversion mechanisms, operating in well-ventilated environments, and limiting the duration of continuous use.

In addition, the study primarily evaluates short-term safety. However, the long-term domestic use of PAW generators poses significant concerns regarding cumulative NO_2 exposure, particularly in poorly ventilated indoor environments. There is also the potential for gradual degradation of internal components, which could affect emission levels over time. Future research should therefore focus on long-duration emission profiling under realistic usage patterns, long-term health risk assessment, and accelerated aging studies to evaluate the device's durability and consistent safety throughout its expected operational lifetime.

Beyond NO_2, further investigations should quantify the emissions and assess the health impacts of other long-lived reactive nitrogen species (RNS) gases that may escape from the plasma reactor into the surrounding air. These include, but are not limited to, nitrous oxide (N_2O), dinitrogen pentoxide (N_2O_5), nitrous acid (HNO_2), and nitric acid (HNO_3) [27], [34]. Understanding the ambient concentrations and health effects of these RNS is essential for ensuring the long-term safety of PAW systems in both domestic and industrial applications.

A summary of the key improvements in the developed flow-through PAW generator compared to the previous version is presented in Table 3. Compared to our previously reported design [8], the newly developed system offers several significant enhancements in both safety and performance. Most notably, the patient leakage current was reduced from 623 µA to just 2.5 µA—well below the IEC DIN EN 60601 safety threshold of 10 µA—ensuring safer direct contact with treated water. In addition, NO_2 emissions measured at a typical user distance (30 cm) were reduced by more than 25-fold, from 7700 ppb to 300 ppb, thereby minimizing respiratory risks during operation. The current NO_2 level remains below Thailand's NAAQS 1-hour exposure limit (170 ppb) when time-weighted, and also below the WHO AQG 24-hour guideline (13.3 ppb), based on continuous operation of the developed flow-through PAW generation system for 20 min.

These improvements were made possible by a redesigned reactor featuring a dual-chamber structure, a gas isolation wall, and an integrated cartridge filter to contain NOx and other hazardous gases. The inclusion of an RCBO provides automatic circuit protection, while the upgraded electrode configuration enhances plasma stability and lowers the risk of leakage current. Together, these advancements represent a substantial step toward making PAW technology safer, more practical, and more suitable for routine domestic applications.

Table 3: Summary of key improvements in the developed flow-through PAW generator compared to the previous version [8].

Aspect	Previous version	Current version (This study)	Improvement
Leakage current	623 µA	2.5 µA	99.6% reduction; below the IEC DIN EN 60601 safety limit of 10 µA
NO_2 emission	7700 ± 1000 ppb	300 ± 200 ppb	25.7-fold reduction; the measured NO_2 level remains below Thailand's NAAQS 1-hour exposure limit (170 ppb) when time-weighted, and also below the WHO AQG 24-hour guideline (13.3 ppb), under continuous operation for 20 min.
Safety features	No integrated RCBO	RCBO installed (IEC 61009-1 compliant)	Enables automatic cutoff at >30 mA leakage within 100 ms
Gas containment design	Single-chamber, no gas barrier	Dual-chamber with gas isolation wall and cartridge filter	Enhanced containment of toxic gases, minimizing air pollution risk
Electrode configuration	Basic electrode setup	Optimized multi-electrode design with safety grounding	Enhanced plasma stability and lower risk of electrical leakage

3.5.3 Nitrite and nitrate residues

The food safety of food ingredients treated with PAW is a critical consideration, as PAW contains dissolved nitrite (NO_2^-) and nitrate ions (NO_3^-). These ions may accumulate in the food matrix and potentially contribute to the formation of nitrosamines, compounds classified as human carcinogens [57]–[59]. Such risks may raise concerns among consumers regarding the safety of PAW-treated food products.

The joint FAO/WHO Expert Committee on Food Additives (JECFA) has established acceptable daily intakes (ADI) for NO_2^- and NO_3^- at 0.06 mg/kg body weight and 3.7 mg/kg body weight, respectively [60]. Therefore, an adult weighing 60 kg can safely consume up to 3.6 mg of nitrite ion and 222 mg of nitrate ion per day.

An analysis was conducted to determine the accumulation of nitrite and nitrate in shucked oyster meat, both untreated and treated by immersion in PAW produced from the flow-through PAW generator for two 10-min cycles. The results showed that residual nitrite levels in untreated and PAW-treated oyster meat were 1.08 mg/kg and 0.82 mg/kg of oyster meat, respectively. Correspondingly, accumulated nitrate levels in untreated and PAW-treated oyster meat were 36.91 mg/kg and 68.32 mg/kg of oyster meat, respectively.

If an adult weighing 60 kg consumes 1 kg of PAW-treated oyster meat, the intake of nitrite and nitrate would be 0.82 mg and 68.32 mg, respectively—both of which are within the established ADI limits. In other words, under these conditions, the consumer could theoretically consume up to 3.2 kg of PAW-treated oyster meat per day without exceeding the ADI for nitrite and nitrate ions.

3.6 *Energy cost*

In addition to contaminant removal efficiency, user safety, food safety, and the initial purchase price of a PAW generation unit, the operational cost of using PAW as a cleaning agent compared to conventional tap water is a critical factor influencing its adoption in household settings. The PAW generation system developed in this study employs ambient air as the plasma-generating gas and tap water as the feed liquid. Consequently, the primary difference in process costs when using PAW as a cleaning agent compared to tap water is the energy cost. This can be calculated based on the total energy consumed by the system and the electricity cost per kilowatt-hour (kWh).

Based on the data presented in Section 3.1, the total electrical power consumption of the flow-through plasma-activated water generator system was 268.4 W. Using an average electricity rate for residential users in Thailand of 4.3 THB/kWh, and considering that the flow-through PAW generator can produce 300 mL of PAW per minute, the electricity cost for producing 1 L of PAW is 0.0641 THB. At an exchange rate of 1 THB = 0.0300 USD, the estimated electricity cost is approximately 0.00192 USD per liter of PAW produced.

4 Conclusions

This study developed and characterized an improved flow-through plasma-activated water generator for household food safety applications, emphasizing enhanced safety, antimicrobial efficacy, and practical feasibility. The developed system demonstrated effective microbial reduction in raw oyster meat, achieving up to 93.5% reduction in total viable counts after two rinse cycles—significantly outperforming sterile distilled water. Furthermore, residual nitrite and nitrate levels in PAW-treated oysters remained well within the acceptable daily intake (ADI) limits established by JECFA, ensuring consumer safety even with high intake scenarios.

Key safety improvements over the previous design include a 99.6% reduction in patient leakage current (from 623 μA to 2.5 μA), and a 25.7-fold reduction in NO_2 emissions (from 7700 ppb to 300 ppb), both of which are now compliant with international safety thresholds such as IEC DIN EN 60601 and Thailand's NAAQS. These improvements were achieved through a dual-chamber plasma reactor design, integrated gas containment features, the installation of an RCBO (IEC 61009-1), and optimization of electrode configurations with safety grounding to enhance plasma stability and reduce the risk of leakage current.

From an environmental perspective, PAW offers a favorable footprint relative to traditional sanitizers, as it is generated on-demand using only tap water and ambient air, without chemical additives or surfactants. It produces minimal residual waste and avoids chemical runoff, making it a sustainable alternative for domestic food decontamination.

In terms of practical feasibility, the developed system operates at an energy cost of approximately 0.00192 USD per liter of PAW produced, making it cost-effective for daily household use. Its compact design, low operating temperature (< 40 °C), and one-

pass generation capability support ease of integration into typical home settings.

Overall, the findings of this study support the use of this improved PAW generator as a safe, efficient, environmentally responsible, and economically viable alternative to conventional chemical sanitizers in household food hygiene.

Acknowledgements

This project is funded by the National Research Council of Thailand (NRCT): Contract number N42A660992.

Author Contributions

P.T.: conceptualization, research design, methodology, investigation, data curation, formal analysis, visualization, validation, writing—original draft preparation, writing—reviewing and editing, resources, supervision, funding acquisition, project administration; M.J.: research design, methodology, investigation, formal analysis, reviewing and editing, resources, supervision, project administration; W.P.: research design, methodology, investigation, formal analysis; J.M.: methodology, formal analysis, resources, supervision, funding acquisition; S.U.: methodology, resources, supervision; D.B.: conceptualization, validation, supervision, funding acquisition; N.P.: research design, methodology, investigation, formal analysis; S.R.: research design, methodology, validation, resources; P.N.: investigation, resources. All authors have read and agreed to the published version of the manuscript.

Conflicts of Interest

The authors declare no conflict of interest.

References

[1] M. Rahman et al., "Plasma-activated water for food safety and quality: A review of recent developments," *International Journal of Environmental Research and Public Health*, vol. 19, no. 11, May 2022, Art. no. 6630, doi: 10.3390/ijerph19116630.

[2] N. N. Misra, T. Naladala, and K. J. Alzahrani, "Design of systems for plasma activated water (PAW) for agri-food applications," *Journal of Physics D: Applied Physics*, vol. 57, no. 49, Dec. 2024, Art. no. 493003, doi: 10.1088/1361-6463/ad77de.

[3] D. Guo, H. Liu, L. Zhou, J. Xie, and C. He, "Plasma-activated water production and its application in agriculture," *Journal of the Science of Food and Agriculture*, vol. 101, no. 12, pp. 4891–4899, Sep. 2021, doi: 10.1002/jsfa.11258.

[4] Y. Yan et al., "Effect of annealing using plasma-activated water on the structure and properties of wheat flour," *Frontiers in Nutrition*, vol. 9, Aug. 2022, doi: 10.3389/fnut.2022.951588.

[5] A. Mai-Prochnow et al., "Interactions of plasma-activated water with biofilms: Inactivation, dispersal effects and mechanisms of action," *npj Biofilms and Microbiomes*, vol. 7, no. 1, Jan. 2021, Art. no. 11, doi: 10.1038/s41522-020-00180-6.

[6] K. -D. Weltmann et al., "Atmospheric pressure plasma jet for medical therapy: Plasma parameters and risk estimation," *Contributions to Plasma Physics*, vol. 49, no. 9, pp. 631–640, Nov. 2009, doi: 10.1002/ctpp.200910067.

[7] A. Lehmann, F. Pietag, and Th. Arnold, "Human health risk evaluation of a microwave-driven atmospheric plasma jet as medical device," *Clinical Plasma Medicine*, vol. 7–8, pp. 16–23, Dec. 2017, doi: 10.1016/j.cpme.2017.06.001.

[8] P. Thana et al., "Plasma-activated water (PAW) decontamination of foodborne bacteria in shucked oyster meats using a compact flow-through generator," *Foods*, vol. 14, no. 9, Apr. 2025, Art. no. 1502, doi: 10.3390/foods14091502.

[9] S. Ungwiwatkul, M. Jaikua, K. Prasertboonyai, P. Thana, A. Tamman, and K. Matra, "Plasma-activated municipal wastewater (PAMW): revolutionizing municipal wastewater into high-value liquid fertilizer for duckweed cultivation through air plasma treatment," *Applied Science and Engineering Progress*, vol. 18, no. 3, Apr. 2025, Art. no. 7791, doi: 10.14416/j.asep.2025.04.002.

[10] P. Thana et al., "A compact pulse-modulation cold air plasma jet for the inactivation of chronic wound bacteria: Development and characterization," *Heliyon*, vol. 5, no. 9, 2019, Art. no. e0245, doi: 10.1016/j.heliyon.2019.e02455.

[11] R. Zhou et al., "Cold atmospheric plasma activated water as a prospective disinfectant: The crucial role of peroxynitrite," *Green*

Chemistry, vol. 20, no. 23, pp. 5276–5284, 2018, doi: 10.1039/C8GC02800A.

[12] G. Bruno, S. Wenske, J.-W. Lackmann, M. Lalk, T. von Woedtke, and K. Wende, "On the liquid chemistry of the reactive nitrogen species peroxynitrite and nitrogen dioxide generated by physical plasmas," *Biomolecules*, vol. 10, no. 12, Dec. 2020, Art. no. 1687, doi: 10.3390/biom10121687.

[13] K. S. Wong, N. S. L. Chew, M. Low, and M. K. Tan, "Plasma-activated water: Physicochemical properties, generation techniques, and applications," *Processes*, vol. 11, no. 7, Jul. 2023, Art. no. 2213, doi: 10.3390/pr11072213.

[14] R. Cui, F. He, J. Miao, and J. Ouyang, "Experimental study on self-pulsing in flow-induced atmospheric pressure plasma jet," *Physics of Plasmas*, vol. 24, no. 10, Oct. 2017, doi: 10.1063/1.4997262.

[15] S. He, J. Li, Y. Qiao, J. Zhao, Q. Li, and L. Dong, "Influence of equivalent resistance on the simulation of self-pulsing discharge by using a circuit model," *The European Physical Journal D*, vol. 76, no. 6, Jun. 2022, Art. no. 99, doi: 10.1140/epjd/s10053-022-00415-5.

[16] M. Zhu et al., "Gliding arc discharge used for water activation: The production mechanism of aqueous NO and its role in sterilization," *Journal of Physics D: Applied Physics*, vol. 56, no. 3, Jan. 2023, Art. no. 035202, doi: 10.1088/1361-6463/aca340.

[17] V. A. Shakhatov and Yu. A. Lebedev, "Radiation spectroscopy in the study of the influence of a helium-nitrogen mixture composition on parameters of DC glow discharge and microwave discharge," *High Temperature*, vol. 50, no. 5, pp. 658–681, Sep. 2012, doi: 10.1134/S0018151X12050173.

[18] Z. Machala, B. Tarabová, D. Sersenová, M. Janda, and K. Hensel, "Chemical and antibacterial effects of plasma activated water: correlation with gaseous and aqueous reactive oxygen and nitrogen species, plasma sources and air flow conditions," *Journal of Physics D: Applied Physics*, vol. 52, no. 3, Jan. 2019, Art. no. 034002, doi: 10.1088/1361-6463/ aae807.

[19] N. K. Kaushik et al., "Biological and medical applications of plasma-activated media, water and solutions," *Biological Chemistry*, vol. 400, no. 1, pp. 39–62, Dec. 2018, doi: 10.1515/hsz-2018-0226.

[20] L. Marcinauskas, R. Uscila, and M. Aikas, "The influence of air flow rates and voltage on the plasma emission spectra and the concentrations of nitrogen oxides produced by gliding arc discharge plasma," *Applied Sciences*, vol. 15, no. 1, Jan. 2025, Art. no. 446, doi: 10.3390/app15010446.

[21] R. P. Joshi and S. M. Thagard, "Streamer-like electrical discharges in water: Part II. Environmental applications," *Plasma Chemistry and Plasma Processing*, vol. 33, no. 1, pp. 17–49, Feb. 2013, doi: 10.1007/s11090-013-9436-x.

[22] S. Theepharaksapan et al., "The potential of plasma-activated water as a liquid nitrogen fertilizer for microalgae cultivation," *IEEE Transactions on Plasma Science*, vol. 52, no. 7, pp. 2392–2402, Jul. 2024, doi: 10.1109/TPS.2024.3362629.

[23] S. V. Tewari, R. J. Kshirsagar, A. Roy, R. Sarathi, A. Sharma, and K. C. Mittal, "Optical emission spectroscopy study on flashover along insulator surface due to particle contamination," *Laser and Particle Beams*, vol. 32, no. 4, pp. 681–689, Dec. 2014, doi: 10.1017/S0263034614000718.

[24] K. Matra, Y. Tanakaran, V. Luang-In, and S. Theepharaksapan, "Enhancement of lettuce growth by PAW spray gliding arc plasma generator," *IEEE Transactions on Plasma Science*, vol. 50, no. 6, pp. 1430–1439, Jun. 2022, doi: 10.1109/TPS.2021.3105733.

[25] K. Matra et al., "Application of electrical breakdown in liquid process on inulin structural transformations," *IEEE Access*, vol. 11, pp. 114777–114789, 2023, doi: 10.1109/ACCESS.2023.3321339.

[26] D. Trunec, Z. Navrátil, J. Tomeková, V. Mazánková, S. Ďurčányová, and A. Zahoranová, "Chemical composition of gaseous products generated by coplanar barrier discharge in air and N_2/O_2 mixtures," *Plasma Sources Science and Technology*, vol. 31, no. 11, Nov. 2022, Art. no. 115011, doi: 10.1088/1361-6595/ac9c8f.

[27] A. Schmidt-Bleker, J. Winter, A. Bösel, S. Reuter, and K.-D. Weltmann, "On the plasma chemistry of a cold atmospheric argon plasma jet with shielding gas device," *Plasma Sources Science and Technology*, vol. 25, no. 1, Feb. 2016, Art. no. 015005, doi: 10.1088/0963-0252/25/1/015005.

[28] A. V. Pipa and J. Ropcke, "Analysis of the mid-infrared spectrum of the exhaust gas from an atmospheric pressure plasma jet (APPJ) working with an argon–air mixture," *IEEE Transactions on Plasma Science*, vol. 37, no. 6, pp. 1000–1003, Jun. 2009, doi: 10.1109/TPS.2009.2013865.

[29] J. Tomeková, S. Kyzek, V. Medvecká, E. Gálová, and A. Zahoranová, "Influence of cold atmospheric pressure plasma on pea seeds: DNA damage of seedlings and optical diagnostics of plasma," *Plasma Chemistry and Plasma Processing*, vol. 40, no. 6, pp. 1571–1584, Nov. 2020, doi: 10.1007/s11090-020-10109-8.

[30] W. Samee et al., "Electrical breakdown in liquid-phase processing on an enhancement of 7-hydroxymitragynine conversion from mitragynine in Mitragyna speciosa (Kratom)," *Heliyon*, vol. 10, no. 17, Sep. 2024, Art. no. e36676, doi: 10.1016/j.heliyon.2024.e36676.

[31] J. Winter et al., "Tracking plasma generated H_2O_2 from gas into liquid phase and revealing its dominant impact on human skin cells," *Journal of Physics D: Applied Physics*, vol. 47, no. 28, Jul. 2014, Art. no. 285401, doi: 10.1088/0022-3727/47/28/285401.

[32] T. J. Johnson, R. L. Sams, S. D. Burton, and T. A. Blake, "Absolute integrated intensities of vapor-phase hydrogen peroxide (H_2O_2) in the mid-infrared at atmospheric pressure," *Analytical and Bioanalytical Chemistry*, vol. 395, no. 2, pp. 377–386, Sep. 2009, doi: 10.1007/s00216-009-2805-x.

[33] A. A. Abdelaziz, T. Ishijima, N. Osawa, and T. Seto, "Quantitative analysis of ozone and nitrogen oxides produced by a low power miniaturized surface dielectric barrier discharge: Effect of oxygen content and humidity level," *Plasma Chemistry and Plasma Processing*, vol. 39, no. 1, pp. 165–185, Jan. 2019, doi: 10.1007/s11090-018-9942-y.

[34] M. Jaikua et al., "Development and characterization of pilot-scale remote cold plasma treatment (RCPT) system for fruit surface decontamination," *Plasma Chemistry and Plasma Processing*, Jun. 2025, doi: 10.1007/s11090-025-10577-w.

[35] M. Laroussi, "Cold plasma in medicine and healthcare: The new frontier in low temperature plasma applications," *Frontiers in Physics*, vol. 8, Mar. 2020, doi: 10.3389/fphy.2020.00074.

[36] P. J. Bruggeman et al., "Plasma–liquid interactions: A review and roadmap," *Plasma Sources Science and Technology*, vol. 25, no. 5, Sep. 2016, Art. no. 053002, doi: 10.1088/0963-0252/25/5/053002.

[37] J. Y. Park and Y. N. Lee, "Solubility and decomposition kinetics of nitrous acid in aqueous solution," *The Journal of Physical Chemistry*, vol. 92, no. 22, pp. 6294–6302, Nov. 1988, doi: 10.1021/j100333a025.

[38] F. Tochikubo, Y. Shimokawa, N. Shirai, and S. Uchida, "Chemical reactions in liquid induced by atmospheric-pressure dc glow discharge in contact with liquid," *Japanese Journal of Applied Physics*, vol. 53, no. 12, Dec. 2014, Art. no. 126201, doi: 10.7567/JJAP.53.126201.

[39] B. Tarabová et al., "Fluorescence measurements of peroxynitrite/peroxynitrous acid in cold air plasma treated aqueous solutions," *Physical Chemistry Chemical Physics*, vol. 21, no. 17, pp. 8883–8896, 2019, doi: 10.1039/C9CP00871C.

[40] K. Panngom et al., "Non-thermal plasma treatment diminishes fungal viability and up-regulates resistance genes in a plant host," *PLoS ONE*, vol. 9, no. 6, Jun. 2014, Art. no. e99300, doi: 10.1371/journal.pone.0099300.

[41] Y. Xu et al., "Plasma-activated water: Candidate hand disinfectant for SARS-CoV-2 transmission disruption," *Heliyon*, vol. 10, no. 15, Aug. 2024, Art. no. e34337, doi: 10.1016/j.heliyon.2024.e34337.

[42] A. Nikolaou et al., "The ratio of reactive oxygen and nitrogen species determines the type of cell death that bacteria undergo," *Microbiological Research*, vol. 292, Mar. 2025, Art. no. 127986, doi: 10.1016/j.micres.2024.127986.

[43] N. Vichiansan et al., "Effect of plasma-activated water (PAW) on the shelf lives of whiteleg shrimp (*Litopenaeus vannamei*) and splendid squid (*Loligo formosana*)," *Food and Bioprocess Technology*, vol. 17, no. 9, pp. 2644–2660, Sep. 2024, doi: 10.1007/s11947-023-03282-z.

[44] E. Tsoukou, M. Delit, L. Treint, P. Bourke, and D. Boehm, "Distinct chemistries define the diverse biological effects of plasma activated water generated with spark and glow plasma discharges," *Applied Sciences*, vol. 11, no. 3, Jan. 2021, Art. no. 1178, doi: 10.3390/app11031178.

[45] R. Zhou et al., "Plasma-activated water: generation, origin of reactive species and

biological applications," *Journal of Physics D: Applied Physics*, vol. 53, no. 30, Jul. 2020, Art. no. 303001, doi: 10.1088/1361-6463/ ab81cf.

[46] W. F. L. M. Hoeben, P. P. van Ooij, D. C. Schram, T. Huiskamp, A. J. M. Pemen, and P. Lukeš, "On the possibilities of straightforward characterization of plasma activated water," *Plasma Chemistry and Plasma Processing*, vol. 39, no. 3, pp. 597–626, May 2019, doi: 10.1007/s11090-019-09976-7.

[47] K. Oehmigen, M. Hähnel, R. Brandenburg, Ch. Wilke, K. -D. Weltmann, and Th. von Woedtke, "The role of acidification for antimicrobial activity of atmospheric pressure plasma in liquids," *Plasma Processes and Polymers*, vol. 7, no. 3–4, pp. 250–257, Mar. 2010, doi: 10.1002/ppap.200900077.

[48] J. Qian, H. Zhuang, M. M. Nasiru, U. Muhammad, J. Zhang, and W. Yan, "Action of plasma-activated lactic acid on the inactivation of inoculated *Salmonella enteritidis* and quality of beef," *Innovative Food Science & Emerging Technologies*, vol. 57, Oct. 2019, Art. no. 102196, doi: 10.1016/j.ifset.2019.102196.

[49] J. Qian, C. Wang, H. Zhuang, M. M. Nasiru, J. Zhang, and W. Yan, "Evaluation of meat-quality and myofibrillar protein of chicken drumsticks treated with plasma-activated lactic acid as a novel sanitizer," *LWT*, vol. 138, Mar. 2021, Art. no. 110642, doi: 10.1016/j.lwt.2020. 110642.

[50] Y.-M. Zhao, M. Oliveira, C. M. Burgess, J. Cropotova, T. Rustad, D.-W. Sun, and B. K. Tiwari, "Combined effects of ultrasound, plasma-activated water, and peracetic acid on decontamination of mackerel fillets," *LWT*, vol. 150, Oct. 2021, Art. no. 111957, doi: 10.1016/ j.lwt.2021.111957.

[51] X. Liu, M. Zhang, X. Meng, Y. Bai, and X. Dong, "Effect of plasma-activated water on *Shewanella putrefaciens* population growth and quality of yellow river carp (*Cyprinus carpio*) fillets," *Journal of Food Protection*, vol. 84, no. 10, pp. 1722–1728, Oct. 2021, doi: 10.4315/JFP -21-031.

[52] K. I. Sallam et al, "Microbial decontamination of beef carcass surfaces by lactic acid, acetic acid, and trisodium phosphate sprays," *BioMed Research International*, vol. 2020, no. 1, Jan. 2020, doi: 10.1155/2020/2324358.

[53] K. M. Killinger, A. Kannan, A. I. Bary, and C. G. Cogger, "Validation of a 2 percent lactic acid antimicrobial rinse for mobile poultry slaughter operations," *Journal of Food Protection*, vol. 73, no. 11, pp. 2079–2083, Nov. 2010, doi: 10.4315/0362-028X-73.11.2079.

[54] M. Sohaib, F. M. Anjum, M. S. Arshad, and U. U. Rahman, "Postharvest intervention technologies for safety enhancement of meat and meat based products; A critical review," *Journal of Food Science and Technology*, vol. 53, no. 1, pp. 19–30, Jan. 2016, doi: 10.1007/ s13197-015-1985-y.

[55] M. Fernández, A. Rodríguez, M. Fulco, T. Soteras, M. Mozgovoj, and M. Cap, "Effects of lactic, malic and fumaric acids on *Salmonella* spp. counts and on chicken meat quality and sensory characteristics," *Journal of Food Science and Technology*, vol. 58, no. 10, pp. 3817–3824, Oct. 2021, doi: 10.1007/s13197-020-04842-3.

[56] D. H. Lee, K.-T. Kim, H. S. Kang, Y.-H. Song, and J. E. Park, "Plasma-assisted combustion technology for NO_x reduction in industrial burners," *Environmental Science & Technology*, vol. 47, no. 19, pp. 10964–10970, Oct. 2013, doi: 10.1021/es401513t.

[57] S. N. Nuñal, K. Jane, M. Monaya, C. Rose, T. Mueda, and S. M. Santander-De Leon, "Microbiological quality of oysters and mussels along its market supply chain," *Journal of Food Protection*, vol. 86, no. 3, Mar. 2023, Art. no. 100063, doi: 10.1016/ j.jfp.2023.100063.

[58] J. Paiva, S. Torres, O. Viana, R. Maggioni, F. Teles, F. R. Queiroga, and P. da Silva, "Oyster (*Crassostrea gasar*) gastrointestinal tract microbiota and immunological responses after antibiotic administration," *Latin American Journal of Aquatic Research*, vol. 47, no. 1, pp. 78–88, Mar. 2019, doi: 10.3856/vol47-issue1-fulltext-9.

[59] A. E. Cabello, R. T. Espejo, and J. Romero, "Tracing *Vibrio parahaemolyticus* in oysters (*Tiostrea chilensis*) using a green fluorescent protein tag," *Journal of Experimental Marine Biology and Ecology*, vol. 327, no. 2, pp. 157–166, Dec. 2005, doi: 10.1016/j.jembe.2005. 06.009.

[60] Y. Zhang et al., "Nitrite and nitrate in meat processing: Functions and alternatives," *Current Research in Food Science*, vol. 6, 2023, Art. no. 100470, doi: 10.1016/j.crfs. 2023.100470.